Root growth of monocotyledons and dicotyledons is limited by different tissues

Anna Petrova, Marina Ageeva, Liudmila Kozlova

Root growth of monocotyledons and dicotyledons is limited by different tissues

Anna Petrova[a], Marina Ageeva[b], Liudmila Kozlova[a,c]*

*Corresponding author: kozlova@kibb.knc.ru, liudmila.kozlova@umontpellier.fr

[a] Laboratory of Plant Cell Growth Mechanisms, Kazan Institute of Biochemistry and Biophysics, FRC Kazan Scientific Center of RAS, 420111, Lobachevsky str., 2/31, Kazan, Russia

[b] Microscopy Cabinet, Kazan Institute of Biochemistry and Biophysics, FRC Kazan Scientific Center of RAS, 420111, Lobachevsky str., 2/31, Kazan, Russia

[c] Mechanics and Civil Engineering Laboratory, University of Montpellier, 860 Rue de St - Priest, 34090, Montpellier, France

SUMMARY

Plant growth and morphogenesis are determined by the mechanical properties of its cell walls. Using atomic force microscopy, we have characterized the dynamics of cell wall elasticity in different tissues in developing roots of several plant species. The elongation growth zone of roots of all species studied was distinguished by a reduced modulus of elasticity of most cell walls compared to the meristem or late elongation zone. Within the individual developmental zones of roots, there were also significant differences in the elasticity of the cell walls of the different tissues, thus identifying the tissues that limit root growth in the different species. In cereals, this is mainly the inner cortex, whereas in dicotyledons this function is performed by the outer tissues – rhizodermis and cortex. These differences result in a different behavior of the roots of these species during longitudinal dissection. Modelling of longitudinal root dissection using measured properties confirmed the difference shown. Thus, the morphogenesis of monocotyledonous and dicotyledonous roots relies on different tissues as growth limiting, which should be taken into account when analyzing the localization of associated molecular events. At the same time, no matrix polysaccharide was found whose immunolabelling in type I or type II cell walls would predict their mechanical properties. However, assessment of the degree of anisotropy of cortical microtubules showed a striking correlation with the elasticity of the corresponding cell walls in all species studied.

Keywords: elongation growth, nano-mechanical properties, primary cell wall, microtubules, growth limiting tissue, root, atomic force microscopy, *Zea mays*, *Secale cereale*, *Glycine max*

SIGNIFICANCE STATEMENT

Juxtaposing the nanomechanical properties of cell walls in growing roots with their composition and the organization of the cytoskeleton revealed key similarities and differences in root morphogenesis in monocots and dicots

INTRODUCTION

Primary cell walls envelope the vast majority of plant cells, with very few exceptions (Esau, 1965). They are composed of polysaccharides with small amounts of proteins and phenolics (Fry, 1988). The growth of plant cells is controlled by the mechanical properties of their cell walls (Coen and Cosgrove, 2023). Growing and non-growing, or growing at different rates, parts of cells and organs are characterized by different mechanical properties of cell walls. In general, the extensibility / softness / compliance of the cell walls of cells and organs that grow faster is higher than that of those that grow slower or do not grow. This has been shown in a variety of plant species and using different methods (atomic force microscopy – Milani et al., 2011; Peaucelle et al., 2015; Majda et al., 2017; Daher et al., 2018; cellular force microscopy – Zerzour et al., 2009; creep test - Cosgrove, 1989; Cosgrove and Li, 1993; Wu et al., 1994; extensometry – Abeysekera and McCully, 1994; Liszkay et al., 2004). However, there are also examples where measured mechanical properties do not directly correlate with growth rate (Silk and Beusmans, 1988; Phyo et al.

2017, Cosgrove, 2022). Furthermore, mechanical properties of the same plant material measured using different methods do not always agree (Bidhendi and Geitmann, 2019, Zhang et al., 2019). The question of the relationship between cell wall composition and mechanical properties remains open.

Two types of primary cell wall are commonly found in higher plants. Type I is characteristic of dicots and non-commelinoid monocots. Type II is characteristic of the commelinids (Carpita, 1996). The basis of the walls in both cases is cellulose. Cellulose microfibrils are considered to be the stiffest component of plant cell walls (the longitudinal modulus of elasticity for cellulose crystals is estimated to be 76-200 GPa and the transverse modulus 10-50 GPa (Lahiji et al., 2010)). Guided by basic ideas about the mechanics of composite materials (Tsai and Hahn, 1980), it can be assumed that the cellulose content, the degree of crystallinity and the arrangement of microfibrils in cell walls should largely determine their mechanics. The direction of cellulose microfibrils in primary cell walls is determined by several mechanisms. The movement of cellulose synthase complexes is controlled by cortical microtubules, which form a rail-like structure on the inner side of the membrane and thus determine the direction of microfibril arrangement in the inner, youngest, layer of the cell wall (Paredez et al., 2006). However, this is a simplistic view, and there is ample evidence that in many cases the direction of microfibrils does not correlate with the direction of microtubules (Baskin et al., 1999; 2004; Hamant et al., 2019; Schneider et al., 2022). In the more superficial layers of the cell wall, passive reorientation of microfibrils along the principal direction of extension occurs during cell growth (Anderson et al., 2010, Zhang et al., 2021).

The non-cellulosic components differ in the different types of primary cell wall. In type I, the major matrix polysaccharides are pectins and xyloglucans, whereas in type II they are represented by glucuronoarabinoxylans and mixed-linkage glucans. Large-scale changes in the proportions and structure of cell wall polysaccharides during cell growth are well documented for many higher plants with different cell wall compositions and for different growth types (coordinated growth – Carpita et al., 1984, Obel et al., 2002, Gibeaut et al., 2005, Petrova et al., 2022, Goldberg and Prat, 1982; Phyo et al., 2017; protrusive growth – Bidhendi et al., 2020; intrusive growth – Majda et al., 2021). In an attempt to summarize these data, the discussion on the role of individual cell wall polysaccharides in realizing plant cell growth in dicotyledonous plants has mainly focused on homogalacturonans and their methylation status (Cosgrove and Anderson, 2020; Haas et al., 2021), and in plants with type II cell walls around changes in the structure of glucuronoarabinoxylans and the presence of mixed-linkage glucan (Vega-Sánchez et al., 2012; Kozlova et al., 2014; Smith-Moritz et al., 2015). Expansins, whose effects on the architecture of the primary cell walls have been extensively studied, are considered to be the primary growth-promoting agents (Sampedro et al., 2015; Wang et al., 2016; Coen and Cosgrove, 2023). So-called "biomechanical hotspots" formed by xyloglucan on cellulose microfibrils are considered targets for the action of expansins, and xyloglucans have therefore also featured in discussions on plant cell growth (Cosgrove, 2022). An additional argument for the involvement of xyloglucans in the regulation of plant growth is the appearance of specific types of these molecules in protrusively growing cells (Peña et al., 2012; Lampugnani et al., 2013; Dardelle et al., 2015; Liu et al., 2015). Thus, there is a considerable body of evidence on the relationship between cell wall composition and cell growth.

The root is an excellent object to study coordinated growth because cells at different stages of development are spatially separated in this organ. Cells from different tissues accelerate and decelerate their growth synchronously. Previously, we have developed a method to assess the elasticity of cell walls in plant internal organs that were not pre-dried, fixed or immersed in hyperosmotic solution (Kozlova et al., 2019; Petrova and Kozlova, 2022). Using this method, we showed the existence of differences in cell wall elasticity in different zones of the maize root and in different tissues (Petrova et al., 2021). We found that one of the stiffest tissues at all stages of maize root development is the inner part of the cortex. At the same time, we did not find any polysaccharide whose immunocytochemical detection in cell walls would predict their mechanical properties. In the present work, we address the following questions: Are there differences between commelinoid monocotyledons and dicotyledons in the distribution and

dynamics of cell wall mechanical properties in the growing root? Is there a parameter that can be used as a proxy to predict mechanical properties in plants with type I and type II cell walls?

RESULTS

Mechanical properties of cell walls in different tissues and developmental zones of the root

Longitudinal sections of rye, maize and soybean primary roots were used to measure the length of cortex cells and to assess the localization of developmental zones along the root axis. Soybean roots were characterized by a longer meristem and a shorter early elongation zone compared to cereals (Table 1).

Table 1. Distribution of root zones in maize, rye and soybean, counted from the junction of the root cap (mm)

	Meristem	Early elongation	Active elongation	Late elongation
Maize	0.0-1.0	1.0-2.0	2.0-6.0	6.0-10.0
Rye	0.0-0.6	0.6-1.2	1.2-2.4	2.4-3.3
Soybean	0.0-1.5	1.5-2.5	2.5-5.5	5.5-9.0

The mechanical properties of fourteen cell wall types of maize roots (Petrova et al., 2021), eleven types of rye roots, and twelve types of soybean roots (Figure 1) were investigated using atomic force microscopy (AFM) on non-fixed, non-embedded and non-dried cross sections taken from the middle of each root zone. In this work, root cross sections obtained with the vibratome were fixed with agarose and examined in liquid using AFM as was described previously (Kozlova et al., 2019; Petrova and Kozlova, 2022).

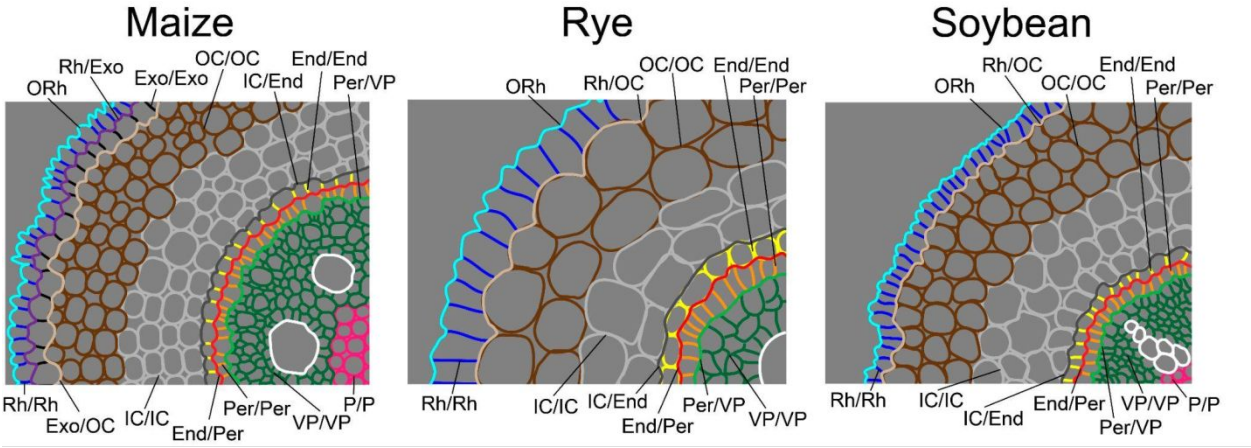

Figure 1. Cell wall types studied in maize (Petrova et al., 2021), rye and soybean. ORh, outer rhizodermis; Rh, rhizodermis; Exo, exodermis; OC, outer cortex; IC, inner cortex; End, endodermis; Per, pericycle; VP, vascular parenchyma; P, pith. Note that both radial longitudinal anticlinal cell walls (Rh/Rh, OC/OC, IC/IC etc.) and tangential longitudinal periclinal cell walls (ORh, Rh/OC, IC/End etc.) were studied with AFM.

The changes in the mechanical properties of rye root cell walls were very similar to those described previously for maize (Petrova et al., 2021). The cell walls of many tissues significantly decreased in apparent Young's modulus during the transition to elongation growth and increased it between the active and late elongation stages. These tissues included rhizodermis, outer and inner cortex, pericycle, and vascular parenchyma (Figure 2, Table 2, 3).

Table 2. Apparent moduli of elasticity of cell walls of rye primary roots (MPa). Mean values ±SD are presented. Lower case letters correspond to significant differences within a column, and upper case letters correspond to significant differences within a row. Means were separated by one-way ANOVA followed by Tukey test at α=0.01.

	Meristem	Early elongation	Elongation	Late elongation
Outer rhizodermis (ORh)	5.6±0.6a B	3.5±0.6a A	3.6±0.5ab A	6.3±1.5a B

Rhizodermis/rhizodermis (Rh/Rh)	5.5±1.3a B	2.9±1.1a A	3.6±0.8ab A	7.9±2.0ab C
Rhizodermis/outer cortex (Rh/OC)	6.8±1.1abc B	5.2±1.1bc A	4.2±0.8abc A	6.6±1.1ab B
Outer cortex/outer cortex (OC/OC)	7.7±1.7bc B	5.4±1.0bc A	4.3±0.7abc A	8.4±2.0ab B
Inner cortex/inner cortex (IC/IC)	8.6±2.2c B	8.2±1.2d AB	5.9±1.5c A	9.9±2.4ab B
Inner cortex/endodermis (IC/End)	7.1±1.4abc AB	5.3±0.9bc A	5.1±1.2bc A	9.6±1.7ab B
Endodermis/endodermis (End/End)	7.1±1.3abc AB	8.3±1.4d AB	4.6±1.1abc A	10.2±1.4b B
Endodermis/pericycle (End/Per)	6.3±1.1ab A	6.2±0.5c A	4.6±1.2bc A	8.7±1.2ab B
Pericycle/pericycle (Per/Per)	6.5±1.1ab B	4.4±1.4ab A	3.8±0.5ab A	8.1±0.8ab B
Pericycle/v. parenchyma (Per/VP)	7.0±0.9abc B	4.1±1.3a A	3.4±0.6ab A	8.8±2.0ab B
V. parenchyma/v. parenchyma (VP/VP)	5.4±1.1a B	3.3±0.7a A	2.6±0.9a A	7.2±1.4ab C

The dynamics described above for most tissues in rye root, including high apparent moduli in the meristem and late elongation zone and lower values in the elongation and early elongation zones, were also characteristic of the rhizodermis (except for the outer wall) and cortex in soybean root. However, the endodermis, pericycle, vascular parenchyma and pith (i.e. all the inner tissues) of soybean root were quite soft in the meristem. The apparent Young's modulus of the cell walls in these tissues increased significantly only at the late elongation stage (Figure 2, Table 3).

Table 3. Apparent moduli of elasticity of cell walls of soybean primary roots (MPa). Mean values ±SD are presented. Lower case letters correspond to significant differences within a column, and upper case letters correspond to significant differences within a row. Means were separated by one-way ANOVA followed by Tukey test at α=0.01.

	Meristem	Early elongation	Elongation	Late elongation
Outer rhizodermis (ORh)	9.7±2.0cd A	9.7±1.0bc A	7.0±0.9ab A	11.0±0.8ab A
Rhizodermis/rhizodermis (Rh/Rh)	9.6±1.1cd B	9.5±0.7b B	5.8±1.1ab A	9.5±1.5ab B
Rhizodermis/outer cortex (Rh/OC)	9.8±1.9cd B	8.8±0.5b AB	6.4±0.6ab A	9.4±1.4ab B
Outer cortex/outer cortex (OC/OC)	10.1±1.1cd B	9.6±1.0b B	6.5±1.7ab A	11.0±2.2ab B
Inner cortex/inner cortex (IC/IC)	12.9±1.0d B	11.6±1.0c AB	7.3±1.2ab A	14.5±3.8b B
Inner cortex/endodermis (IC/End)	7.6±0.8abc A	7.8±0.8b A	7.7±1.3b A	13.8±1.0ab B
Endodermis/endodermis (End/End)	8.6±0.7bc A	9.0±1.0b AB	7.4±0.4ab A	11.6±1.8ab B
Endodermis/pericycle (End/Per)	7.1±1.2abc A	5.5±0.7a A	6.1±1.0ab A	12.5±1.1ab B
Pericycle/pericycle (Per/Per)	5.2±0.5ab A	5.0±1.3a A	4.4±0.7a A	10.8±1.1ab B
Pericycle/v. parenchyma (Per/VP)	4.7±0.6a A	4.6±0.6a A	4.5±1.1a A	10.1±0.2ab B
V. parenchyma/v. parenchyma (VP/VP)	4.8±0.4a A	4.1±0.6a A	5.2±0.9ab A	10.6±1.0ab B
Pith/pith (P/P)	4.7±0.6a A	4.8±0.6a A	4.7±1.0ab A	8.2±0.8a B

Differences in the elasticity of the cell walls of different tissues within the same root zone were also found. In the rye meristem, the cell walls of the outer and inner cortex were the stiffest, whereas the rhizodermis and vascular parenchyma were significantly softer. The cell walls of the inner cortex remained the stiffest both in the early elongation zone and in the elongation zone. The general increase in elastic moduli in the

late elongation zone of the rye root was accompanied by an almost complete disappearance of the differences in mechanical properties between the cell walls of the different tissues (Table 2).

In the meristem and early elongation zone of soybean roots, the rhizodermis and cortex had the stiffest cell walls, while the vascular parenchyma and pith had the softest. A general decrease in cell wall modulus was observed in the elongation zone. Differences between the individual tissues almost disappeared with the exception of the endodermis. Similarly, the overall increase in cell wall modulus in the soybean root between the elongation zone and the late elongation zone left almost no significant differences between the individual tissues (Table 3).

The cell walls in the meristem of all three species were stiffer than those in the zones of early elongation and elongation (Figure 2). However, in cereals, rye and maize, the stiffest tissue was the inner cortex, whereas in soybean, all outer tissues, including the rhizodermis, had stiffer cell walls than those located in the central cylinder, vascular parenchyma and pith. Most of the cell walls in all three species had the lowest Young's moduli in the elongation zone. In the late elongation zone, the cell walls of most tissues became much stiffer than in the active elongation zone.

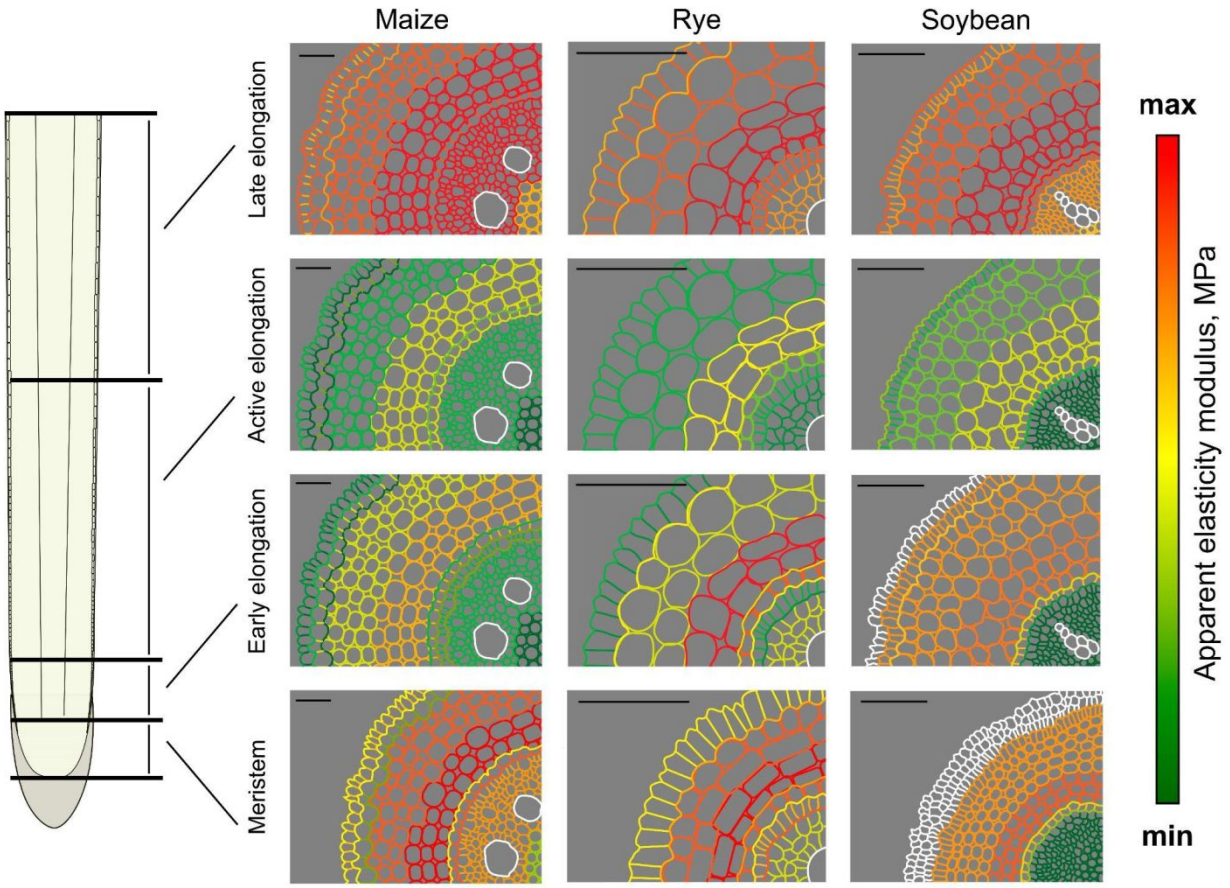

Figure 2. Apparent elastic moduli of different cell walls of maize, rye and soybean roots at different stages of development. Scale bars correspond to 100 µm. Schematic drawings are made from real cross sections of each species. The tissues not examined – xylem and root cap – are shown in white. The colour coding is based on the maximum and minimum values of the apparent Young's moduli for each species separately.

Cereal and dicot roots behaved differently when the root was cut longitudinally (Figure 3). Longitudinal cutting of a maize root resulted in a structure resembling a needle eye: two halves of the maize root were bent inwards. Soybean roots showed an outward curvature after cutting. Longitudinal dissection of the cylindrical plant organs leads to a partial release of the stresses they are carrying. Outward curvature corresponds to longitudinal tensional stress in the outer tissues (Kutschera and Niklas, 2007), while inward

curvature indicates higher stress in the inner tissues. The highest longitudinal stress, in turn, corresponds to the growth-limiting tissue (Tomos et al., 1989). Thus, the observed differences in the behavior of maize and soybean roots after longitudinal cutting may indicate that these species have different root growth-limiting tissues.

To test whether the measured mechanical properties of the cell walls were consistent with this root behavior, a computational model was constructed. To simulate a root dissection, half of the root was modelled on a tissue scale using the finite element method (Figure 3). The arrangement and dimensions of the tissues and root zones corresponded to the real ones in maize and soybean. However, only those tissues whose mechanical properties were measured were modelled. Each tissue in each root zone was assigned the properties of its cell walls and was modelled as an isotropic material. Once the initial model was built, a pressure of 0.6 MPa was applied from the inside to all of its outer planes, including the "cut" plane, to simulate turgor.

After the application of turgor, deformations occurred in the root models of both species (Figure 3). The soybean root half deviated from its original vertical position in the direction corresponding to an outward bend. The maize root half model deformed in the opposite direction, corresponding to an inward bend of the root after dissection. The complex shape acquired by the root half corresponded to the needle eye appearance that the real maize root acquires after cutting when it comes into contact with the other half.

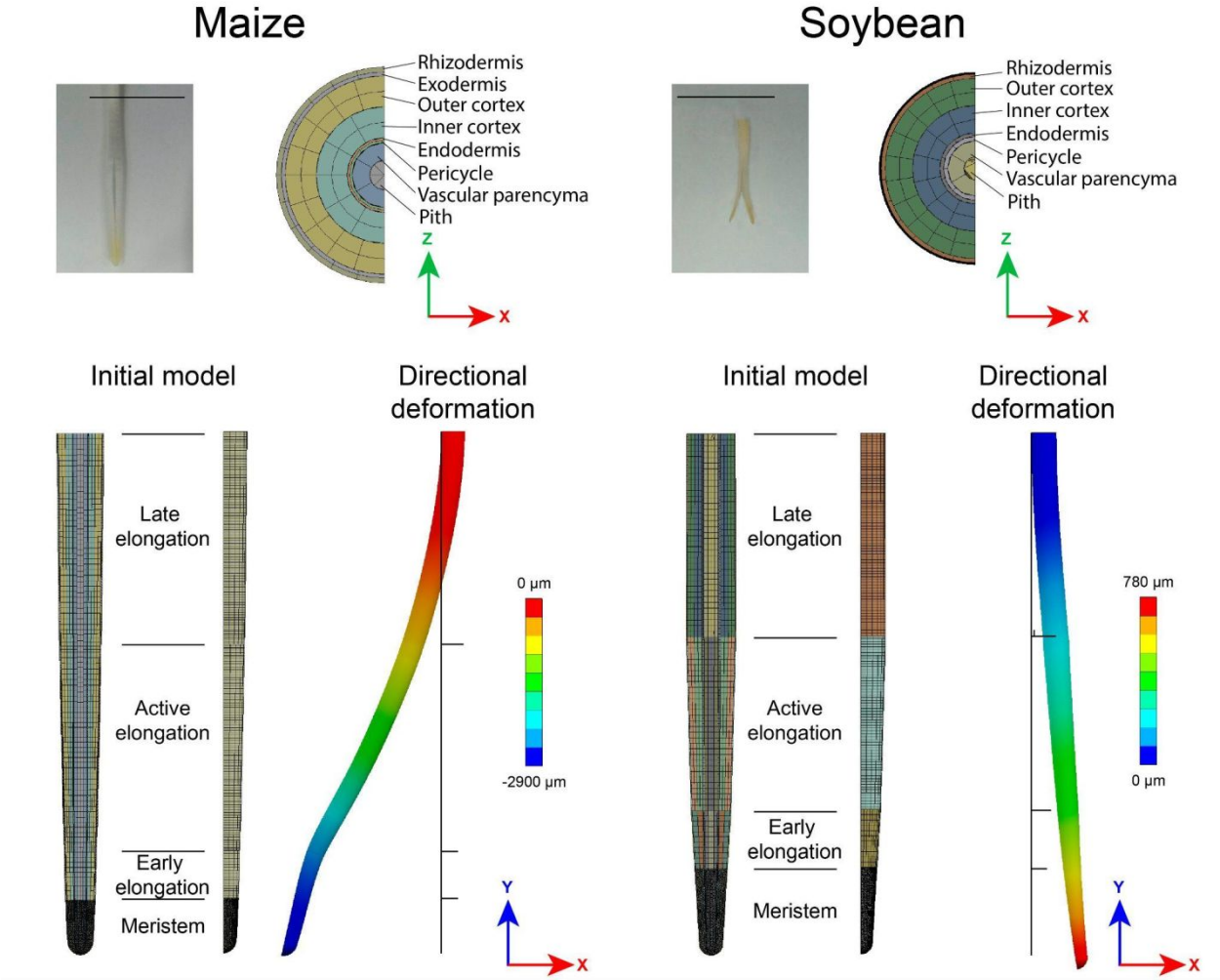

Figure 3. Maize and soybean primary roots cut longitudinally. In the top row, photographs of cut roots and cross sections (Y-axis view) of modelled root halves. In the bottom row, initial models (Z-axis and X-axis views) and deformation of modelled root halves in the X-direction after application of turgor pressure to the initial model. The black lines in the directional deformation images show the position and zonation of the initial model.

Immunochemical characterization of the polysaccharide composition of root cell walls in monocotyledonous and dicotyledonous plants

The dynamics of polysaccharides in type II cell walls of maize and rye roots during their development has been studied and described previously (Petrova et al., 2021; 2022). Soybean root cell walls contained a classical set of polysaccharides characteristic of type I cell walls. They were rich in cellulose, xyloglucan and pectins (Figures S1-S3). Antibodies to xylan (LM11, McCartney et al., 2005) and glucuronoxylan (LM28, Cornuault et al., 2015) labelled secondary cell walls emerging in the xylem in the late elongation zone as expected (Figure S4), and antibodies to xylogalacturonan (LM8, Willats et al., 2004) were bound by root mucilage (Figure S4). The diversity of immunocytochemically detectable polysaccharide motifs in soybean roots was significantly lower than that in cereal roots (Figures S1-S4, Petrova et al., 2021; 2022). Antibodies LM7, LM9, LM21, and LM27 (Willats et al., 2001; Clausen et al., 2004; Marcus et al., 2010; Cornuault et al., 2015) did not bind to soybean roots.

A number of polysaccharides have been suggested to be involved in the regulation of cell wall mechanics. We focused on their labelling in the early elongation zone in the roots of three species, as the mechanical differences were most pronounced in this zone (Figure 2; Tables 2, 3; Petrova et al., 2021).

Xyloglucan, which together with cellulose is thought to be involved in the formation of "biomechanical hotspots" and the realization of expansin action (Park and Cosgrove, 2012), was detected in the early elongation zone of maize, rye and soybean roots using two antibodies – LM25 for xyloglucan (Pedersen et al., 2012) and CCRC-M1 for fucosylated xyloglucan (Puhlmann et al., 1994) (Figure 4).

In cereals, labelling with antibodies to xyloglucan was tissue specific (Figure 4). For example, maize inner and outer cortex differed in their labelling with the LM25 antibody. However, the mechanical properties of these cell walls were similar (Figure 2, Petrova et al., 2021). In contrast, pith and outer cortex cell walls in the early elongation zone of the maize root were equally labelled with LM25 (Figure 4), whereas their mechanical properties differed dramatically (Table 2). Similar examples were found in rye. Strong labelling with LM25 antibody was observed in the cell walls of vascular parenchyma and outer cortex of rye root, whereas their apparent Young's moduli were statistically different (Table 2). The epitope of CCRC-M1 was found only in root mucilage and protoxylem in the early elongation zone of maize roots and in mucilage and rhizodermis in the same zone of rye roots (Figure 4). Thus, the immunolabelling of fucosylated xyloglucans did not reflect the diversity of mechanical properties of cereal cell walls. In soybean, both fucosylated and non-fucosylated xyloglucans were detected in the cell walls of all tissues. The signals were not stronger or weaker in tissues with different mechanical properties. For example, the softest tissue at this stage in the soybean root was the vascular parenchyma and the stiffest was the inner cortex (Table 3). The intensity of their labelling appeared to be the same (Figure 4). The intensity of antibody binding to cell walls remained more or less constant in other zones of the soybean root (Figure S3), despite significant changes in the moduli (Table 3).

Given the anisotropic nature of root growth, it is useful to compare the labelling of transverse anticlinal and longitudinal periclinal cell walls in longitudinal root sections, as their mechanical properties are also known to differ in the axial organs (Peaucelle et al., 2015; Daher et al., 2018). The anticlinal cell walls in cereal roots appeared to carry more xyloglucan (LM25) epitope than the periclinal cell walls (Figure 4), but in soybean root this labelling appeared to be uniform in anticlinal and periclinal cell walls.

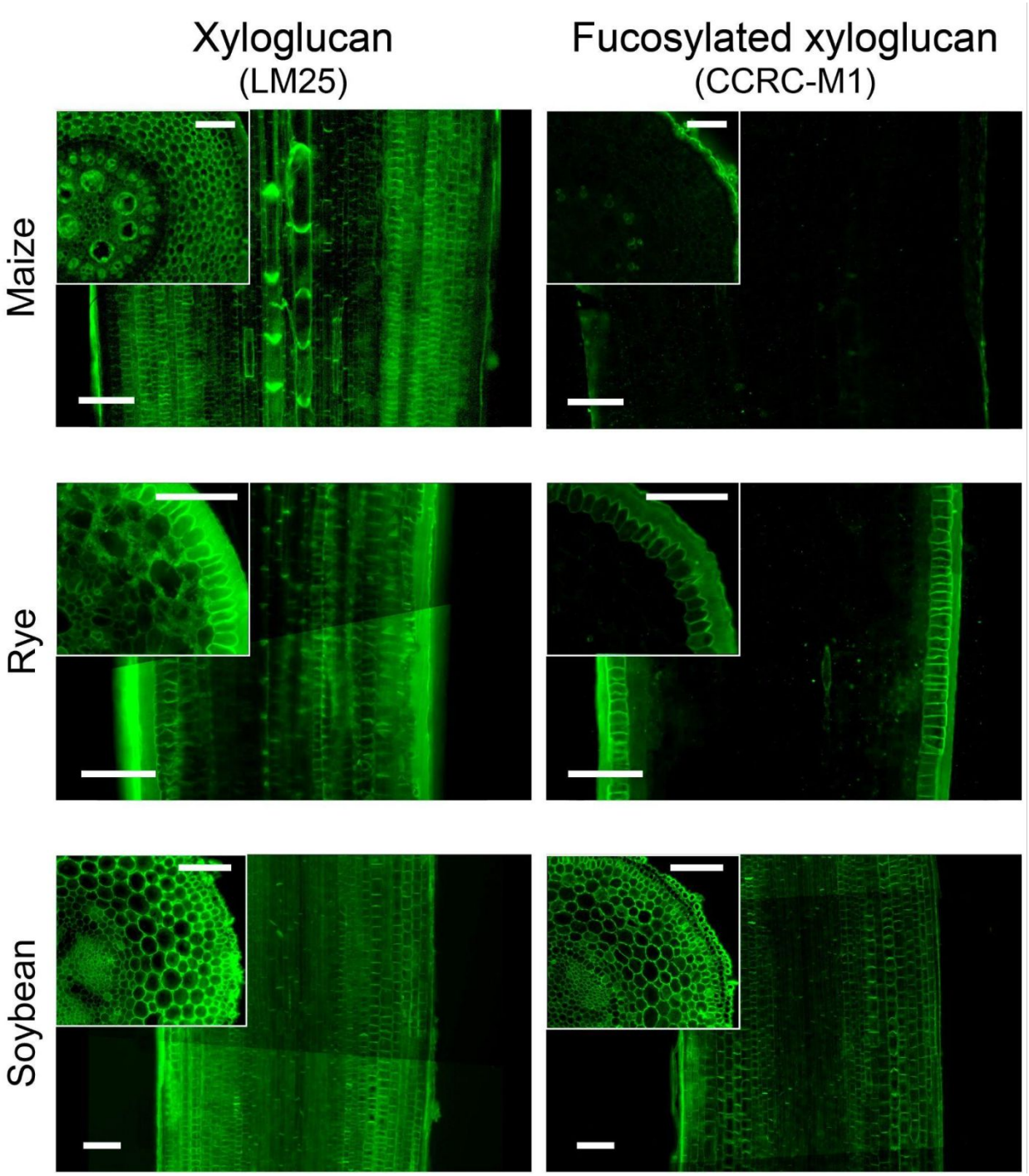

Figure 4. Fluorescence micrographs of maize, rye and soybean primary roots longitudinal and cross sections in the early elongation zone immunolabelled with LM25 (xyloglucan) or CCRC-M1 (fucosylated xyloglucan) antibodies. Scale bars are 100 µm.

The degree of methylation of homogalacturonans, as well as the protein agents capable of modifying it (pectin methylesterases and their inhibitors), are often considered as regulators of cell wall mechanical properties in dicotyledonous plants (Peaucelle et al., 2015; Hocq et al., 2017; Daher et al., 2018). However, labelling with LM19 or LM20 antibodies specific for low and high methylated homogalacturonans, respectively (Verhertbruggen et al., 2009), also did not match the distribution of Young's modulus in cell walls of different tissues in the early elongation zones of rye, maize or soybean roots (Figure 5). The labelling of anticlinal and periclinal cell walls also appeared similar in each of the three plant species.

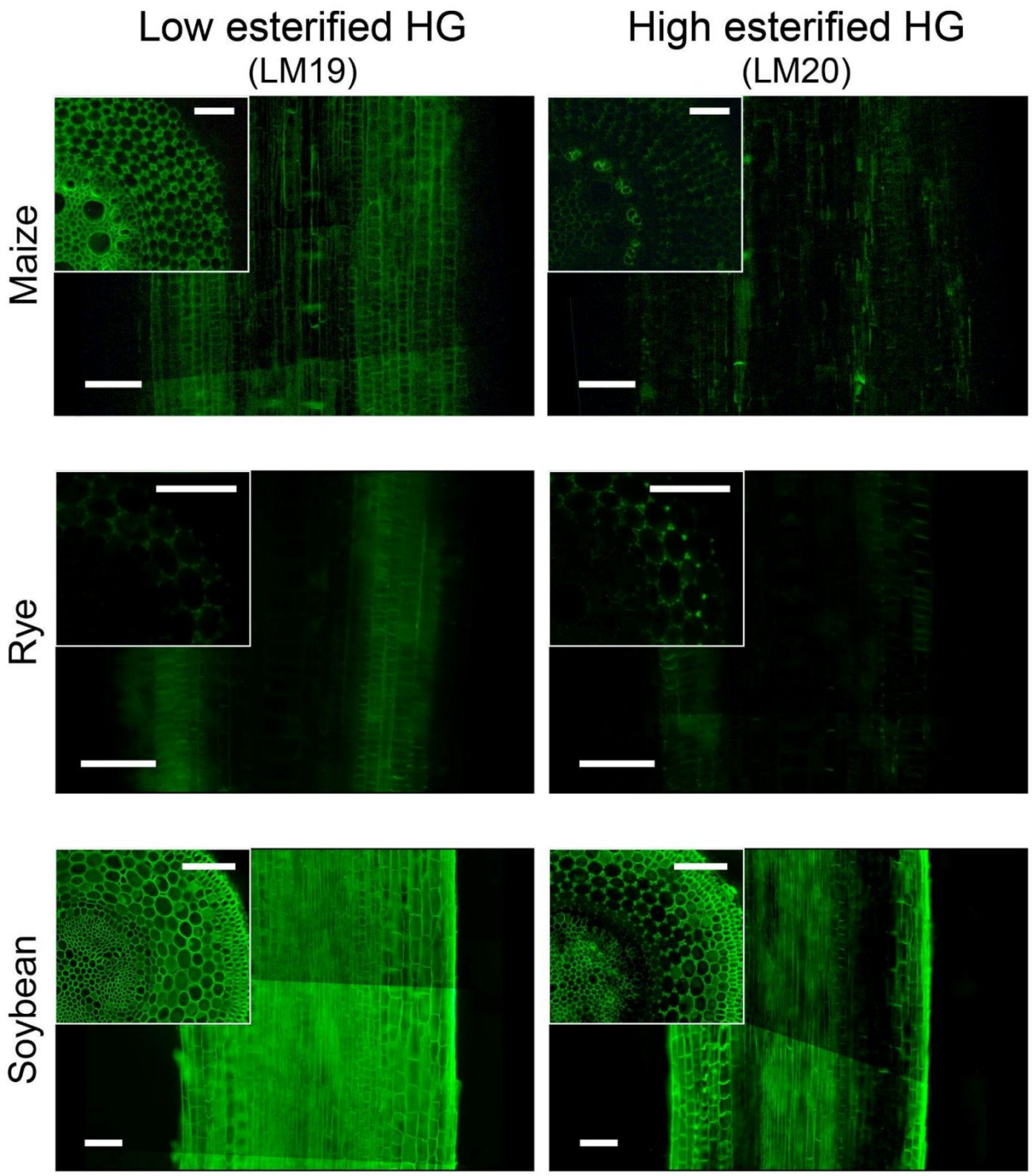

Figure 5. Fluorescence micrographs of maize, rye and soybean primary roots longitudinal and cross sections in the early elongation zone immunolabelled with LM19 (low esterified homogalacturonan (HG)) or LM20 (high esterified homogalacturonan (HG)) antibodies. Scale bars are 100 µm.

The orientation of cellulose microfibrils is also often considered as a factor determining the mechanical properties of plant cell walls (Suslov and Verbelen, 2006). The orientation of cellulose microfibrils in the newly deposited cell wall layer can be inferred by analysing the orientation of cortical microtubules. We labelled microtubules on central longitudinal root sections of three species with specific antibodies (Figure 6A) and assessed their anisotropy in the early elongation zone (Figure 6B) using the FibrilTool (Boudaoud et al., 2014). The anisotropy score takes values from 0 to 1, where 0 corresponds to no ordering (pure isotropic arrays) and 1 to perfectly ordered, i.e., parallel fibrils (purely anisotropic arrays). Note that since the study was performed on central longitudinal sections, only radial anticlinal cell faces were available for analysis.

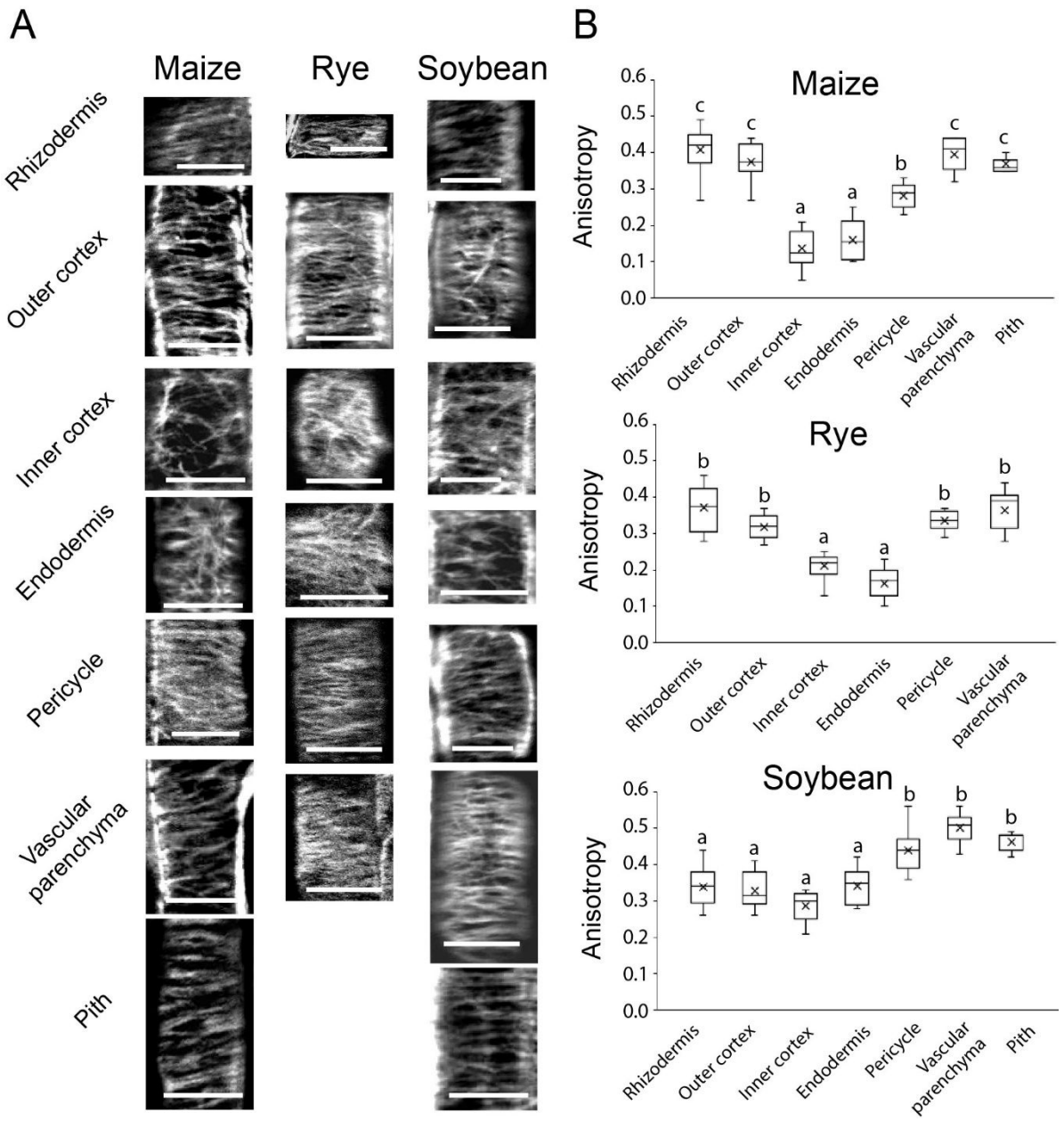

Figure 6. Cortical microtubule organization in radial anticlinal cell faces in the early elongation zone of maize, rye, and soybean primary roots. A – Micrographs of cortical microtubules in different species and tissues labelled with DM1A antibody. Scale bars are 10 μm. B – Anisotropy scores of cortical microtubules in different species and tissues. Boxes correspond to a 25-75th percentile, middle line to median value, cross to mean value, upper and lower whiskers to maximum and minimum values respectively. Different letters indicate significant differences within a species, determined by one-way ANOVA followed by Tukey's test at α=0.01.

In maize, the most chaotically organized microtubules were observed in the radial anticlinal cell faces of the inner cortex and endodermis cells. Much higher levels of anisotropy, i.e. more ordered cortical microtubules, were observed in the rhizodermis, outer cortex, vascular parenchyma and pith cells (Figure 6). In rye, the inner cortex and endodermis also had the least ordered cortical microtubules compared to tissues at the root periphery and in the central cylinder (Figure 6). Soybean roots differed from maize and rye roots in that the rhizodermis, outer and inner cortex, and endodermis had lower values of the anisotropy score compared to the pericycle, vascular parenchyma, and pith, i.e. the outer tissues were characterized by less ordered microtubules than the inner tissues (Figure 6).

The anisotropy score showed a strong inverse correlation with the apparent elastic moduli of radial anticlinal cell walls in the same tissues for all three species. The correlation coefficient was -0.91 for maize, -0.95 for rye, and -0.98 for soybean. This means that in the early elongation zone of maize, rye and soybean roots, more chaotically organized cortical microtubules corresponded to stiffer cell walls, whereas more aligned and anisotropic microtubules corresponded to softer cell walls.

DISCUSSION

Elongation growth in monocotyledonous and dicotyledonous roots correlates with a decrease in cell wall elasticity

Although there are numerous examples of AFM-measured cell wall elasticity being consistent with the presence and rate of growth of plant cells and tissues (Milani et al., 2011; Majda et al., 2017; Peaucelle et al., 2015; Daher et al., 2018; Petrova et al., 2021), the debate continues as to whether nanoindentation results reflect cell wall extensibility (Zhang et al., 2019). Here, by measuring elastic moduli in the longitudinal (axial) direction, we have shown that in rye and soybean, two plant species belonging to different taxa, in many tissues the cell walls are significantly stiffer in the root meristem than in the early elongation zone. The lowest longitudinal elastic moduli were observed in the active elongation zone. The cessation of elongation growth was accompanied by an increase in the apparent Young's moduli in many root tissues (Table 2, 3, Figure 2). This is in agreement with our previous results for maize roots (Petrova et al., 2021). The dynamics are also consistent with those described for maize root by Beusman and Silk (1988) for changes in bending modulus along the root length, although not exactly the same for root length millimeters. However, the authors pointed out that the bending modulus profile can vary significantly depending on the cultivation temperature and differs between fast and slow growing roots. Since the described dynamics of changes in the mechanical properties of cell walls has already been found in three species of higher plants belonging to different taxa, it can be assumed that it may be universal for growing roots.

Root growth in rye and maize is limited by internal tissues, while in soybean it is limited by external tissues

In addition to the changes in mechanical properties between root zones, both rye and soybean, as well as maize (Petrova et al., 2021) showed significant differences in the elasticity of the cell walls of the different tissues within the zones (Table 2, 3, Figure 2). The stiffest tissue in cereal roots was the inner cortex, whereas in soybean the stiffest tissues were the rhizodermis, outer cortex and inner cortex. A higher stiffness of the cortex tissues compared to the stele was also recently shown in barley roots (Fusi et al., 2022). The stiffest tissue limits organ growth (Tomos et al., 1989), so the growth limiting tissues may differ between species according to our results. Further confirmation of the above differences between monocotyledonous and dicotyledonous plants was provided by the method of longitudinal cutting. After bisection, soybean and maize roots behave differently: the maize root halves bend inwards, while the soybean root halves bend outwards (Figure 3). The tendency of maize roots to bend inwards after dissection has been shown previously (Fan et al., 2006). Inward bending corresponds to the presence of longitudinally tensioned inner tissues, whereas outward bending indicates tension in the outer layers. Tension, in turn, should occur in the stiffest tissue due to its restraining role (Kutschera and Niklas, 2007). Futher confirmation that the identified mechanical properties of the cell walls are realistic came from a computer simulation. The simulated root halves, in which the properties of all tissues corresponded to those of their cell walls, bent inwards in maize and outwards in soybean when turgor was applied (Figure 3).

Why is the establishment of growth limiting tissues important? For example, it is known that in maize roots the inner cortex is the most sensitive tissue to auxin and ethylene (Baluška et al., 2001), consistent with its function as a growth limiting tissue. It is therefore reasonable to assume that in soybean it is the outer tissues that should have this sensitivity. In another much better studied dicotyledon, *Arabidopsis*,

the rhizodermis is known to be particularly sensitive to auxin, at least in the gravitropic response (Swarup et al., 2005), whereas in maize the rhizodermis can be partially removed and neither normal root growth nor its gravitropism is altered (Bjorkman and Cleland, 1991). It can be suggested that, in general, the molecular events that determine growth rate should be localized primarily in the growth limiting tissues. These tissues should be studied with particular attention when results such as single cell transcriptomes are analyzed in the context of elongation growth.

The question remains as to why growth limiting tissues differ between monocots and dicots. This may be due to differences in the structure of the roots themselves and root systems in general. Cereals have no secondary growth in their roots, the phloem and xylem are represented by scattered poles, the roots themselves tend to be thinner and organized into a fibrous root system, in contrast to dicotyledons, which have mainly a tap root system, are capable of secondary growth and consequently have a more pronounced vascular system (Esau, 1965).

Labelling of cell wall components with antibodies does not correlate with mechanical properties of cell walls in early elongation zone of roots, while microtubule anisotropy does

The idea of a polysaccharide, or a specific substructure of the cell wall polysaccharide, that directly affects the mechanical properties of the cell wall and is exploited by plants to regulate them seems both simple and logical. Among others, the association of high and low methylated homogalacturonan with more and less stiff cell walls, respectively, has the largest amount of factual evidence (Peuacelle et al., 2015; Daher et al., 2018; Jonsson et al., 2021).

At the same time, it is known that in pollen tubes, in contrast to the vegetative organs of dicotyledons, the opposite is true: high methylated homogalacturonan is characteristic for a softer cell wall at the pollen tube tip, and low methylated for a stiffer one in the distal part of the tube (Geitmann and Parre, 2004; Parre and Geitmann, 2005; Bolduc et al., 2006; Vogler et al., 2013; Hocq et al., 2020). Here we have shown that in the roots of neither cereals nor dicotyledon plant there is a strict association between the occurrence of high or low methylated homogalacturonan and more or less elastic cell walls (Figure 2, 5). No differences were also found in the labelling of anticlinal and periclinal cell walls with the corresponding antibodies in the early elongation zone (Figure 5), although the anisotropic nature of root growth predicts that the expansion of the former will be significantly less pronounced than that of the latter.

Similarly, the distribution of xyloglucan epitopes in cell walls was not related to the mechanical properties of these cell walls in plants with either type I or type II cell walls (Figure 4), despite existing hypotheses (Park and Cosgrove, 2012).

The use of atomic force microscopy in combination with microscopy-based immunocytochemistry of individual cell wall components to identify the structures responsible for the mechanical properties of the walls is very attractive, as these techniques have a similar resolution range. However, due to the inherent limitations of both these approaches (for a brief discussion of this issue, see Kozlova et al., 2019 and Petrova et al., 2021), direct correlation of their results can only be made with great caution.

In this study, a strong negative correlation was found between the degree of cortical microtubule anisotropy in the radial anticlinal cell faces (Figure 6) and the apparent modulus of elasticity of the corresponding cell walls in the early elongation zone of roots of three plant species. This means that the lower the anisotropy of the cortical microtubules, i.e. the more chaotically they are arranged, the stiffer the corresponding cell wall will be. Conversely, softer cell walls correspond to higher anisotropy (higher order) of cortical microtubules in the zone of early elongation of roots of all three species (Figs. 2, 6). A similar pattern has already been shown in *Arabidopsis* shoot apical meristems. Their central part, characterized by slow isodiametric growth and stiffer cell walls than in the fast and anisotropically growing flanks (Milani et al., 2011), is also distinguished by its microtubules being chaotically arranged and rapidly changing their direction, whereas in the flanks the microtubules are more ordered (Burian et al., 2013).

Cortical microtubules are well known to play an important role in controlling the mechanical anisotropy of cells by regulating the deposition of cellulose microfibrils (Chan et al., 2011; Chan, 2012; Sampathkumar et al., 2014; Hamant et al., 2019). Analyses of microtubule orientation in different tissues of growing maize and *Arabidopsis* roots have already been performed many times (Baluška et al., 1992; Baluška et al., 1993; Blancaflor and Hasenstein, 1995; Liang et al., 1997; Baskin et al. 1999; Baluška et al., 2001; Baskin et al., 2004), but they relied on subjective evaluation and were mostly qualitative. At the same time, the main parameter evaluated (and still evaluated in most cytoskeleton-related works) was the angle of microtubule inclination, although it is clear that this metric is almost meaningless when the degree of anisotropy is low (Boudaoud et al., 2014). The above work can be summarized as follows: in the elongation zone of *Arabidopsis* and maize roots, microtubules and cellulose microfibrils are oriented transversely, i.e. perpendicular to the root axis (Baluška et al., 1992; Liang et al., 1997; Baskin et al., 1999; 2004). In the late elongation zone, microtubules become oblique and then parallel to the root axis, but cellulose microfibrils continue to be deposited perpendicular to this axis, demonstrating an example of dissociation between microtubules and cellulose patterns (Baskin et al., 1999; 2004). Random organization of microtubules has been observed in the quiescent centre of the maize root (Baluška et al., 1992). The zone of early elongation in our work corresponds to the transition zone in the work of F. Baluška and J.-P. Verbelen (Baluška et al., 2001; Verbelen et al., 2006). In this zone, microtubules change their orientation from chaotic to transverse. In different tissues, this process begins and ends at different times, depending on the duration of divisions in these tissues (Baluška et al., 2001; Verbelen et al., 2006). Thus, the differences in the degree of microtubule anisotropy observed in the zone of early elongation in our work reflect differences in the dynamics of this process between different root tissues and in different species. A lower degree of cortical microtubule anisotropy presumably provides for a more chaotic deposition of cellulose microfibrils in the inner cortex of cereal roots and in the cortex and rhizodermis of soybean roots, which in turn allows these tissues to perform their growth-limiting functions.

Cortical microtubules, cellulose microfibrils, cell wall stiffness and cell wall stress distribution form a feedback loop (Hamant et al., 2019; Sampathkumar, 2020), but the primary stimulus cannot be identified. For example, for one of the most extensively studied objects, the pavement cells of *Arabidopsis* cotyledons that acquire a jigsaw puzzle shape, different groups refer to pectin biochemistry (Haas et al., 2020), local differences in cell wall stiffness (Majda et al., 2017), compressive or tensile stresses generated in the cell wall (Bidhendi et al., 2019; Belteton et al., 2021) as the primary stimulus for triggering the feedback loop and consequently morphogenesis. The already complex view of this multi-component feedback loop is further complicated by the fact that it does not always function continuously and can be disrupted. For example, at early stages of *Arabidopsis* pavement cell development, the correlation between the movement of cellulose synthase complexes and the location of microtubules is quite low (Schneider et al., 2022). It also has been shown in maize and *Arabidopsis* roots, that microtubule orientation does not always correlate with cellulose microfibril orientation, in both control and oryzalin-treated plants (Baskin et al., 1999; 2004). Changes in the stress distribution pattern do not always lead to microtubule reorientation in *Arabidopsis* hypocotyls (Robinson and Kuhlemeer, 2018). The functioning of this feedback loop certainly requires further investigation, but here, using three plant species, we have shown that in the early elongation zone of the root, the degree of cortical microtubule anisotropy can be used as a proxy to predict the mechanical properties of the cell wall.

METHODS

Plant material

Seeds of soybean (*Glycine max*, cultivar Donskaya 9 elita), rye (*Secale cereale*, cultivar Tatarskaya 1), and maize (*Zea mays*, cultivar Interkras 375) were sterilized with 0.35% NaOCl solution (10 min), washed three times with distilled water and then grown hydroponically in the dark at 27°C for 4 d (soybean and maize) or 2 d (rye). To characterize root stresses *in planta*, one apical cm of maize and soybean roots was cut longitudinally with a blade and the resulting bends were photographed.

Determination of soybean root zonation pattern

The distribution of developmental zones along maize and rye roots has been characterized previously (Kozlova et al., 2012; Petrova et al., 2022). For a similar study on soybean roots, longitudinal sections obtained with a Leica VT1000S vibratome (Leica Biosystems, Wetzlar, Germany) were used. The sections were observed and photographed using a Leica DM1000 epifluorescence microscope (Leica Biosystems, Germany). Cortex cell lengths were measured in a single file in every 100 µm of root length starting from the junction with the root cap, then the data were averaged within each mm of root length. Cell lengths were measured on photomicrographs using ImageJ2 Fiji software (https://imagej.net/).

Immunolabelling of cell wall polysaccharides

Transverse and longitudinal sections of roots were prepared using a Leica VT1000S vibratome (Leica Biosystems, Wetzlar, Germany) at a blade speed of 0.65 mm s^{-1} and a blade frequency of 70 Hz. Sections were incubated for 10 min in a 4% (w/v) paraformaldehyde solution prepared on 0.2 M phosphate-buffered saline (PBS, pH 7.2). Immunolabelling procedures were performed using INRA-RU2 (INRA, Nantes, France); LM5, LM6, LM8, LM9, LM11, LM19, LM20, LM21, LM25, LM26, LM27, LM28 (Leeds University, Leeds, UK), and CCRC-M1 (CarboSource, Athens, GA, USA) as primary antibodies (Table S3). For immunolocalization, sections were blocked with 0.2M PBS containing 2% (w/v) bovine serum albumin (BSA) for 30 min at room temperature, incubated with one of the primary monoclonal antibodies diluted 1:5 (LM5, LM6, LM8, LM9, LM11, LM19, LM20, LM21, LM25, LM26, LM27, LM28, CCRC-M1) or 1:3 (INRA-RU2) for 1.5 h at room temperature, then washed three times with PBS and incubated with secondary anti-rat (LM5, LM6, LM8, LM9, LM11, LM19, LM20, LM21, LM25, LM26, LM27, LM28) or anti-mouse (INRA-RU2, CCRC-M1) IgGs conjugated to fluorescein isothiocyanate (FITC, Sigma-Aldrich, St. Louis, MO, USA) diluted 1:100 in PBS for 1 h at room temperature in the dark. Treatment with primary antibody was omitted for the negative controls. After incubation with antibodies, the sections were washed four times in PBS and twice in water. For cellulose staining, sections were incubated in Carbotrace^{TM}680 (Ebba Biotech, Solna, Sweden) 1:1000 solution in PBS, then washed three times in PBS and twice in water. Sections were observed using a Leica DM1000 epifluorescence microscope (Leica Biosystems, Wetzlar, Germany) equipped with a mercury lamp and appropriate filter cubes (excitation filter 460-500 nm, barrier filter 512-542 nm for FITC conjugated antibodies; excitation filter 540-580 nm, barrier filter 608-683 nm for Carbotrace^{TM}680).

Imaging of cortical microtubules and analysis of their orientation

Maize, rye and soybean root segments were fixed in 4% paraformaldehyde solution prepared on microtubule-stabilizing buffer (MSB: 50 mM PIPES, 5 mM EGTA, 1 mM $MgSO_4$, 1% glycerol, 0.25% v/v Triton X-100, pH 6.9) for 1 h. After fixation, longitudinal sections (50 µm thick) were prepared using a Leica VT1000S vibratome (Leica Biosystems, Wetzlar, Germany). For immunolocalization, sections were blocked with Tris buffer (TBS: 150 mM NaCl, 20 mM Tris-HCl, 0.25% v/v Triton-X100, pH 7.4) containing 2% (w/v) bovine serum albumin (BSA) for 30 min at room temperature. The sections were then incubated with primary antibody against α-tubulin DM1A (Thermo Fisher Scientific, Waltham, MA, USA) diluted 1:100 in TBS overnight at 4°C. Sections were washed three times with TBS and incubated with secondary anti-mouse IgG H&L (Texas Red, Thermo Fisher Scientific, Waltham, MA, USA) diluted 1:500 in TBS for 1 hour at room temperature in the dark. Sections were observed using an LSM-510 confocal laser scanning microscope (Zeiss, Oberkochen, Germany) with a 543 nm laser and LP560 emission filter.

The FibrilTool plug-in (Boudaoud et al., 2014) for ImageJ Fiji (https://imagej.net/) was used to analyze cortical microtubule orientation in radial cell walls of different root tissues (rhizodermis, outer cortex, inner cortex, endodermis, pericycle, vascular parenchyma and pith) in the early elongation zone of maize, rye and soybean roots. Pearson's correlation coefficient was used to assess the correlation between microtubule orientation and mechanical properties of radial cell walls.

Atomic force microscopy

Measurements of the mechanical properties of the cell walls were made using AFM on agarose-embedded 300-400 µm thick cross sections of different zones of rye and soybean roots. The types of cell wall examined for each species are shown in Figure 1. Sections were taken near the middle of each zone using a Leica VT1000S vibratome (Leica Biosystems, Wetzlar, Germany). AFM experiments were performed at room temperature in a liquid cell using an NTEGRA Prima microscope (NT-MDT, Zelenograd, Russia). The AFM HybriD mode was used to obtain the elasticity map using FMG01 tips (NT-MDT, Zelenograd, Russia, with a typical resonance frequency of 60 kHz, mean spring constant of 2.8 N m^{-1}, and tip radius of 10 nm). The detailed protocol of sample preparation, measurements and data analysis can be found in Petrova and Kozlova (2022).

Finite element modeling

The responses of maize and soybean primary roots to longitudinal dissection were modelled using ANSYS 2020 R2 (ANSYS Inc., Canonsburg, PA, USA). The model represented half of a sectioned root consisting of seven tissue layers for soybean and eight for maize in four developmental zones of the root (i.e. meristem, early elongation, active elongation and late elongation) (Figure 3). Microphotographs of cross sections of roots taken at every mm of their length were used to determine the dimensions of individual tissues using ImageJ2 Fiji software (https://imagej.net/). Each tissue was modelled as an isotropic material with a Young's modulus equal to that of its cell walls, as measured in the present study for soybean and in Petrova et al. (2021) for maize. Some tissues had cell walls whith different properties on different sides of the cells. In this case, the modulus of elasticity for these tissues was calculated as the average of the corresponding cell walls. For example, the modulus of elasticity of the endoderm was the average of the moduli measured for the outer tangential (IC/End), radial (End/End) and inner tangential (End/Per) cell walls of the endoderm. Roots were modelled using 100 µm hexagonal elements for early, active and late elongation zones and 20 µm square elements for the meristem. The mesh independence of the results was tested by using meshes of different coarseness. Displacement of the upper surface of the modelled roots was not allowed, while the rest of the root could be displaced in either direction. The applied turgor pressure was 0.6 MPa (Petrova et al., 2021).

Statistics

Ten soybean roots were used to determine the zonation pattern. Four biological replicates for each antibody were used for immunocytochemical analyses. The mechanical properties of each tissue in each developmental zone were examined in five biological replicates. Means $\pm$ standard deviation between the biological replicates are presented. Mean separation was performed by ANOVA followed by the Tukey test at $\alpha = 0.01$ using the SPSS software package (v.21, IBM Corp., Armonk, NY, USA).

AUTHOR CONTRIBUTIONS

LK designed the research; AP and MA conducted the experiments; LK and AP analyzed the data; LK and AP wrote the manuscript. All authors reviewed and edited the manuscript.

ACKNOWLEDGMENTS

We would like to express our gratitude to Prof. Paul Knox (University of Leeds, UK), Dr. Marie-Christine Ralet and Dr. Fabienne Guillon (French National Institute for Agricultural Research, Nantes, France) for kindly providing the antibodies used in this study. Rye seeds were provided by Prof. Mira Ponomareva (Tatar Scientific Research Institute of Agriculture, Kazan, Russia). Maize seeds were provided by Dr. Dmitry Suslov (Saint-Petersburg State University, Russia). This study was partially supported by the Russian Science Foundation (grant number 18-14-00168, LK; and grant number 21-74-10131, AP). Part of the study (confocal microscopy, AP and MA) was carried out with financial support from the government assignment for FRC Kazan Scientific Center of RAS.

CONFLICT OF INTEREST

The authors declare no conflict of interest.

References

Abeysekera, R.M. and Mccully, M.E. (1994) The epidermal surface of the maize root-tip .3. isolation of the surface and characterization of some of its structural and mechanical-properties. *New Phyt*, **127**, 321-333. https://doi.org/10.1111/j.1469-8137.1994.tb04283.x

Anderson, C.T., Carroll, A., Akhmetova, L. and Somerville, C. (2010) Real-time imaging of cellulose reorientation during cell wall expansion in Arabidopsis roots. *Plant Physiol*, **152**, 787-796. https://doi.org/10.1104/pp.109.150128

Baluška, F., Parker, J.S., Barlow, P.W. (1992) Specific patterns of cortical and endoplasmic microtubules associated with cell growth and tissue differentiation in roots of maize (*Zea mays* L.). *J Cell Sci*, **103**, 191-200. https://doi.org/10.1242/jcs.103.1.191

Baluška, F., Brailsford, R.W., Hauskrecht, M., Jackson, M.B. and Barlow, P.W. (1993) Cellular dimorphism in the maize root cortex: involvement of microtubules, ethylene and gibberellin in the differentiation of cellular behaviour in postmitotic growth zones. *Bot Acta*, **106**, 394-403. https://doi.org/10.1111/j.1438-8677.1993.tb00766.x

Baluška, F., Volkmann, D. and Barlow, P.W. (2001) A polarity crossroad in the transition growth zone of maize root apices: cytoskeletal and developmental implications. *J Plant Growth Regul*, **20**, 170-181. https://doi.org/10.1007/s003440010013

Baskin, T.I., Meekes, H.T., Liang, B.M. and Sharp, R.E. (1999) Regulation of growth anisotropy in well-watered and water-stressed maize roots. II. Role of cortical microtubules and cellulose microfibrils. *Plant Physiol*, **119**, 681-692. https://doi.org/10.1104/pp.119.2.681

Baskin, T.I., Beemster, G.T., Judy-March, J.E. and Marga, F. (2004) Disorganization of cortical microtubules stimulates tangential expansion and reduces the uniformity of cellulose microfibril alignment among cells in the root of Arabidopsis. *Plant Physiol*, **135**, 2279-2290. https://doi.org/10.1104/pp.104.040493

Belteton, S.A., Li, W., Yanagisawa, M., Hatam, F.A., Quinn, M.I., Szymanski, M.K., Marley, M.W., Turner, J.A. and Szymanski, D.B. (2021) Real-time conversion of tissue-scale mechanical forces into an interdigitated growth pattern. *Nat Plants*, **7**, 826-841. https://doi.org/10.1038/s41477-021-00931-z

Beusmans, J.M. and Silk, W.K. (1988) Mechanical properties within the growth zone of corn roots investigated by bending experiments. II. Distributions of modulus and compliance in bending. *Am J Bot*, **75**, 996-1002. https://doi.org/10.2307/2443767

Bidhendi, A.J., Altartouri, B., Gosselin, F.P. and Geitmann, A. (2019) Mechanical stress initiates and sustains the morphogenesis of wavy leaf epidermal cells. *Cell Rep*, **28**, 1237-1250 e1236. https://doi.org/10.1016/j.celrep.2019.07.006

Bidhendi, A.J. and Geitmann, A. (2019) Methods to quantify primary plant cell wall mechanics. *J Exp Bot*, **70**, 3615-3648. https://doi.org/10.1093/jxb/erz281

Bidhendi, A.J., Chebli, Y. and Geitmann, A. (2020) Fluorescence visualization of cellulose and pectin in the primary plant cell wall. *J Microsc*, **278**, 164-181. https://doi.org/10.1111/jmi.12895

Bjorkman, T. and Cleland, R.E. (1991) Root growth regulation and gravitropism in maize roots does not require the epidermis. *Planta*, **185**, 34-37. https://doi.org/

Blancaflor, E.B. and Hasenstein, K.H. (1995) Time course and auxin sensitivity of cortical microtubule reorientation in maize roots. *Protoplasma*, **185**, 72-82. https://doi.org/10.1007/BF01272755

Bolduc, J.E., Lewis, L.J., Aubin, C.E. and Geitmann, A. (2006) Finite-element analysis of geometrical factors in micro-indentation of pollen tubes. *Biomech Model Mechanobiol*, **5**, 227-236. https://doi.org/10.1007/s10237-005-0010-1

Boudaoud, A., Burian, A., Borowska-Wykret, D., Uyttewaal, M., Wrzalik, R., Kwiatkowska, D. and Hamant, O. (2014) FibrilTool, an ImageJ plug-in to quantify fibrillar structures in raw microscopy images. *Nat Protoc*, **9**, 457-463. https://doi.org/10.1038/nprot.2014.024

Burian, A., Ludynia, M., Uyttewaal, M., Traas, J., Boudaoud, A., Hamant, O. and Kwiatkowska, D. (2013) A correlative microscopy approach relates microtubule behaviour, local organ geometry, and cell growth at the Arabidopsis shoot apical meristem. *J Exp Bot*, **64**, 5753-5767. https://doi.org/10.1093/jxb/ert352

Carpita, N.C. (1984) Cell wall development in maize coleoptiles. *Plant Physiol*, **76**, 205-212. https://doi.org/10.1104/pp.76.1.205

Carpita, N.C. (1996) Structure and biogenesis of the cell walls of grasses. *Annu Rev Plant Physiol Plant Mol Biol*, **47**, 445-476. https://doi.org/10.1146/annurev.arplant.47.1.445

Chan, J., Eder, M., Crowell, E.F., Hampson, J., Calder, G. and Lloyd, C. (2011) Microtubules and CESA tracks at the inner epidermal wall align independently of those on the outer wall of light-grown Arabidopsis hypocotyls. *J Cell Sci*, **124**, 1088-1094. https://doi.org/10.1242/jcs.086702

Chan, J. (2012) Microtubule and cellulose microfibril orientation during plant cell and organ growth. *J Microsc*, **247**, 23-32. https://doi.org/10.1111/j.1365-2818.2011.03585.x

Clausen, M.H., Ralet, M.C., Willats, W.G., McCartney, L., Marcus, S.E., Thibault, J.F. and Knox, J.P. (2004) A monoclonal antibody to feruloylated-(1-->4)-beta-D-galactan. *Planta*, **219**, 1036-1041. https://doi.org/10.1007/s00425-004-1309-3

Coen, E. and Cosgrove, D.J. (2023) The mechanics of plant morphogenesis. *Science*, **379**, eade8055. https://doi.org/10.1126/science.ade8055

Cornuault, V., Buffetto, F., Rydahl, M.G., Marcus, S.E., Torode, T.A., Xue, J., Crepeau, M.J., Faria-Blanc, N., Willats, W.G., Dupree, P., Ralet, M.C. and Knox, J.P. (2015) Monoclonal antibodies indicate low-abundance links between heteroxylan and other glycans of plant cell walls. *Planta*, **242**, 1321-1334. https://doi.org/10.1007/s00425-015-2375-4

Cosgrove, D.J. (1989) Characterization of long-term extension of isolated cell walls from growing cucumber hypocotyls. *Planta*, **177**, 121-130. https://doi.org/10.1007/BF00392162

Cosgrove, D.J. and Li, Z.C. (1993) Role of expansin in cell enlargement of oat coleoptiles - Analysis of developmental gradients and photocontrol. *Plant Physiol*, **103**, 1321-1328. https://doi.org/10.1104/pp.103.4.1321

Cosgrove, D.J. and Anderson, C.T. (2020) Plant cell growth: Do pectins drive lobe formation in Arabidopsis pavement cells? *Curr Biol*, **30**, 660-662. https://doi.org/10.1016/j.cub.2020.04.007

Cosgrove, D.J. (2022) Building an extensible cell wall. *Plant Physiol*, **189**, 1246-1277. https://doi.org/10.1093/plphys/kiac184

Daher, F.B., Chen, Y.J., Bozorg, B., Clough, J., Jonsson, H. and Braybrook, S.A. (2018) Anisotropic growth is achieved through the additive mechanical effect of material anisotropy and elastic asymmetry. *Elife*, **7**. https://doi.org/10.7554/eLife.38161

Dardelle, F., Le Mauff, F., Lehner, A., Loutelier-Bourhis, C., Bardor, M., Rihouey, C., Causse, M., Lerouge, P., Driouich, A. and Mollet, J.C. (2015) Pollen tube cell walls of wild and domesticated tomatoes contain arabinosylated and fucosylated xyloglucan. *Ann Bot*, **115**, 55-66. https://doi.org/10.1093/aob/mcu218

Esau, K. (1965) *Plant anatomy* 2nd edition edn. New York: John Wiley & Sons.

Fan, L., Linker, R., Gepstein, S., Tanimoto, E., Yamamoto, R. and Neumann, P.M. (2006) Progressive inhibition by water deficit of cell wall extensibility and growth along the elongation zone of maize roots is related to increased lignin metabolism and progressive

stelar accumulation of wall phenolics. *Plant Physiol*, **140**, 603-612. https://doi.org/10.1104/pp.105.073130

Fry, S.C. (1988) *The growing plant cell wall: Chemical and metabolic analysis*: Longman Scientific & Technical.

Fusi, R., Rosignoli, S., Lou, H., Sangiorgi, G., Bovina, R., Pattem, J.K., Borkar, A.N., Lombardi, M., Forestan, C., Milner, S.G., Davis, J.L., Lale, A., Kirschner, G.K., Swarup, R., Tassinari, A., Pandey, B.K., York, L.M., Atkinson, B.S., Sturrock, C.J., Mooney, S.J., Hochholdinger, F., Tucker, M.R., Himmelbach, A., Stein, N., Mascher, M., Nagel, K.A., De Gara, L., Simmonds, J., Uauy, C., Tuberosa, R., Lynch, J.P., Yakubov, G.E., Bennett, M.J., Bhosale, R. and Salvi, S. (2022) Root angle is controlled by EGT1 in cereal crops employing an antigravitropic mechanism. *Proc Natl Acad Sci USA*, **119**, e2201350119. https://doi.org/10.1073/pnas.2201350119

Geitmann, A. and Parre, E. (2004) The local cytomechanical properties of growing pollen tubes correspond to the axial distribution of structural cellular elements. *Sex Plant Reprod*, **17**, 9-16. https://doi.org/10.1007/s00497-004-0210-3

Gibeaut, D.M., Pauly, M., Bacic, A. and Fincher, G.B. (2005) Changes in cell wall polysaccharides in developing barley (Hordeum vulgare) coleoptiles. *Planta*, **221**, 729-738. https://doi.org/10.1007/s00425-005-1481-0

Goldberg, R. and Prat, R. (1982) Involvement of cell wall characteristics in growth processes along the mung bean hypocotyl. *Plant Cell Physiol*, **23**, 1145-1154. https://doi.org/10.1093/oxfordjournals.pcp.a076455

Haas, K.T., Wightman, R., Meyerowitz, E.M. and Peaucelle, A. (2020) Pectin homogalacturonan nanofilament expansion drives morphogenesis in plant epidermal cells. *Science*, **367**, 1003-1007. https://doi.org/10.1126/science.aaz5103

Haas, K.T., Wightman, R., Peaucelle, A. and Hofte, H. (2021) The role of pectin phase separation in plant cell wall assembly and growth. *Cell Surf*, **7**, 100054. https://doi.org/10.1016/j.tcsw.2021.100054

Hamant, O., Inoue, D., Bouchez, D., Dumais, J. and Mjolsness, E. (2019) Are microtubules tension sensors? *Nat Commun*, **10**, 2360. https://doi.org/10.1038/s41467-019-10207-y

Hocq, L., Pelloux, J. and Lefebvre, V. (2017) Connecting homogalacturonan-type pectin remodeling to acid growth. *Trends Plant Sci*, **22**, 20-29. https://doi.org/10.1016/j.tplants.2016.10.009

Hocq, L., Guinand, S., Habrylo, O., Voxeur, A., Tabi, W., Safran, J., Fournet, F., Domon, J.M., Mollet, J.C., Pilard, S., Pau-Roblot, C., Lehner, A., Pelloux, J. and Lefebvre, V. (2020) The exogenous application of AtPGLR, an endo-polygalacturonase, triggers pollen tube burst and repair. *Plant J*, **103**, 617-633. https://doi.org/10.1111/tpj.14753

Jonsson, K., Lathe, R.S., Kierzkowski, D., Routier-Kierzkowska, A.L., Hamant, O. and Bhalerao, R.P. (2021) Mechanochemical feedback mediates tissue bending required for seedling emergence. *Curr Biol*, **31**, 1154-1164 e1153. https://doi.org/10.1016/j.cub.2020.12.016

Kozlova, L.V., Snegireva, A.V. and Gorshkova, T.A. (2012) Distribution and structure of mixed linkage glucan at different stages of elongation of maize root cells. *Russ J Plant Physiol*, **59**, 339-347. https://doi.org/10.1134/S1021443712030090

Kozlova, L.V., Ageeva, M.V., Ibragimova, N.N. and Gorshkova, T.A. (2014) Arrangement of mixed-linkage glucan and glucuronoarabinoxylan in the cell walls of growing maize roots. *Ann Bot-London*, **114**, 1135-1145. https://doi.org/10.1093/aob/mcu125

Kozlova, L., Petrova, A., Ananchenko, B. and Gorshkova, T. (2019) Assessment of primary cell wall nanomechanical properties in internal cells of non-fixed maize roots. *Plants-Basel*, **8**. https://doi.org/10.3390/plants8060172

Kutschera, U. and Niklas, K.J. (2007) The epidermal-growth-control theory of stem elongation: an old and a new perspective. *J Plant Physiol*, **164**, 1395-1409. https://doi.org/10.1016/j.jplph.2007.08.002

Lampugnani, E.R., Moller, I.E., Cassin, A., Jones, D.F., Koh, P.L., Ratnayake, S., Beahan, C.T., Wilson, S.M., Bacic, A. and Newbigin, E. (2013) In vitro grown pollen tubes of Nicotiana alata actively synthesise a fucosylated xyloglucan. *PLoS One*, **8**, e77140. https://doi.org/10.1371/journal.pone.0077140

Liang, B.M., Sharp, R.E. and Baskin, T.I. (1997) Regulation of growth anisotropy in well-watered and water-stressed maize roots (I. Spatial distribution of longitudinal, radial, and tangential expansion rates). *Plant Physiol*, **115**, 101-111. https://doi.org/10.1104/pp.115.1.101

Liszkay, A., van der Zalm, E. and Schopfer, P. (2004) Production of reactive oxygen intermediates (O(2)(.-), H(2)O(2), and (.)OH) by maize roots and their role in wall loosening and elongation growth. *Plant Physiol*, **136**, 3114-3123. https://doi.org/10.1104/pp.104.044784

Liu, L., Paulitz, J. and Pauly, M. (2015) The presence of fucogalactoxyloglucan and its synthesis in rice indicates conserved functional importance in plants. *Plant Physiol*, **168**, 549-560. https://doi.org/10.1104/pp.15.00441

Majda, M., Grones, P., Sintorn, I.M., Vain, T., Milani, P., Krupinski, P., Zagorska-Marek, B., Viotti, C., Jonsson, H., Mellerowicz, E.J., Hamant, O. and Robert, S. (2017) Mechanochemical polarization of contiguous cell walls shapes plant pavement cells. *Dev Cell*, **43**, 290-304 e294. https://doi.org/10.1016/j.devcel.2017.10.017

Majda, M., Kozlova, L., Banasiak, A., Derba-Maceluch, M., Iashchishyn, I.A., Morozova-Roche, L.A., Smith, R.S., Gorshkova, T. and Mellerowicz, E.J. (2021) Elongation of wood fibers combines features of diffuse and tip growth. *New Phytol*, **232**, 673-691. https://doi.org/10.1111/nph.17468

Marcus, S.E., Blake, A.W., Benians, T.A., Lee, K.J., Poyser, C., Donaldson, L., Leroux, O., Rogowski, A., Petersen, H.L., Boraston, A., Gilbert, H.J., Willats, W.G. and Knox, J.P. (2010) Restricted access of proteins to mannan polysaccharides in intact plant cell walls. *Plant J*, **64**, 191-203. https://doi.org/10.1111/j.1365-313X.2010.04319.x

McCartney, L., Marcus, S.E. and Knox, J.P. (2005) Monoclonal antibodies to plant cell wall xylans and arabinoxylans. *J Histochem Cytochem*, **53**, 543-546. https://doi.org/10.1369/jhc.4B6578.2005

Milani, P., Gholamirad, M., Traas, J., Arneodo, A., Boudaoud, A., Argoul, F. and Hamant, O. (2011) In vivo analysis of local wall stiffness at the shoot apical meristem in Arabidopsis using atomic force microscopy. *Plant J*, **67**, 1116-1123. https://doi.org/10.1111/j.1365-313X.2011.04649.x

Obel, N., Porchia, A.C. and Scheller, H.V. (2002) Dynamic changes in cell wall polysaccharides during wheat seedling development. *Phytochem*, **60**, 603-610. https://doi.org/10.1016/s0031-9422(02)00148-6

Paredez, A.R., Somerville, C.R. and Ehrhardt, D.W. (2006) Visualization of cellulose synthase demonstrates functional association with microtubules. *Science*, **312**, 1491-1495. https://doi.org/10.1126/science.1126551

Park, Y.B. and Cosgrove, D.J. (2012) A revised architecture of primary cell walls based on biomechanical changes induced by substrate-specific endoglucanases. *Plant Physiol*, **158**, 1933-1943. https://doi.org/10.1104/pp.111.192880

Parre, E. and Geitmann, A. (2005) Pectin and the role of the physical properties of the cell wall in pollen tube growth of Solanum chacoense. *Planta*, **220**, 582-592. https://doi.org/10.1007/s00425-004-1368-5

Peaucelle, A., Wightman, R. and Höfte, H. (2015) The control of growth symmetry breaking in the Arabidopsis hypocotyl. *Curr Biol*, **25**, 1746-1752. https://doi.org/10.1016/j.cub.2015.05.022

Pedersen, H.L., Fangel, J.U., McCleary, B., Ruzanski, C., Rydahl, M.G., Ralet, M.C., Farkas, V., von Schantz, L., Marcus, S.E., Andersen, M.C., Field, R., Ohlin, M., Knox, J.P., Clausen, M.H. and Willats, W.G. (2012) Versatile high resolution oligosaccharide microarrays for plant glycobiology and cell wall research. *J Biol Chem*, **287**, 39429-39438. https://doi.org/10.1074/jbc.M112.396598

Peña, M.J., Kong, Y., York, W.S. and O'Neill, M.A. (2012) A galacturonic acid-containing xyloglucan is involved in Arabidopsis root hair tip growth. *Plant Cell*, **24**, 4511-4524. https://doi.org/10.1105/tpc.112.103390

Petrova, A., Gorshkova, T. and Kozlova, L. (2021) Gradients of cell wall nano-mechanical properties along and across elongating primary roots of maize. *J Exp Bot*, **72**, 1764-1781. https://doi.org/10.1093/jxb/eraa561

Petrova, A. and Kozlova, L. (2022) Characterizing mechanical properties of primary cell wall in living plant organs using atomic force microscopy. *J Vis Exp*, 63904. https://doi.org/10.3791/63904

Petrova, A., Sibgatullina, G., Gorshkova, T. and Kozlova, L. (2022) Dynamics of cell wall polysaccharides during the elongation growth of rye primary roots. *Planta*, **255**, 108. https://doi.org/10.1007/s00425-022-03887-2

Phyo, P., Wang, T., Kiemle, S.N., O'Neill, H., Pingali, S.V., Hong, M. and Cosgrove, D.J. (2017) Gradients in wall mechanics and polysaccharides along growing inflorescence stems. *Plant Physiol*, **175**, 1593-1607. https://doi.org/10.1104/pp.17.01270

Puhlmann, J., Bucheli, E., Swain, M.J., Dunning, N., Albersheim, P., Darvill, A.G. and Hahn, M.G. (1994) Generation of monoclonal antibodies against plant cell-wall polysaccharides. I. Characterization of a monoclonal antibody to a terminal alpha-(1-->2)-linked fucosyl-containing epitope. *Plant Physiol*, **104**, 699-710. https://doi.org/10.1104/pp.104.2.699

Robinson, S. and Kuhlemeier, C. (2018) Global compression reorients cortical microtubules in arabidopsis hypocotyl epidermis and promotes growth. *Curr Biol*, **28**, 1794-1802 e1792. https://doi.org/10.1016/j.cub.2018.04.028

Sampathkumar, A., Krupinski, P., Wightman, R., Milani, P., Berquand, A., Boudaoud, A., Hamant, O., Jonsson, H. and Meyerowitz, E.M. (2014) Subcellular and supracellular mechanical stress prescribes cytoskeleton behavior in Arabidopsis cotyledon pavement cells. *Elife*, **3**, e01967. https://doi.org/10.7554/eLife.01967

Sampathkumar, A. (2020) Mechanical feedback-loop regulation of morphogenesis in plants. *Development*, **147**. https://doi.org/10.1242/dev.177964

Sampedro, J., Guttman, M., Li, L.C. and Cosgrove, D.J. (2015) Evolutionary divergence of beta-expansin structure and function in grasses parallels emergence of distinctive primary cell wall traits. *Plant J*, **81**, 108-120. https://doi.org/10.1111/tpj.12715

Schneider, R., Ehrhardt, D.W., Meyerowitz, E.M. and Sampathkumar, A. (2022) Tethering of cellulose synthase to microtubules dampens mechano-induced cytoskeletal organization in Arabidopsis pavement cells. *Nat Plants*, **8**, 1064-1073. https://doi.org/10.1038/s41477-022-01218-7

Silk, W.K. and Beusmans, J.M. (1988) Mechanical properties within the growth zone of corn roots investigated by bending experiments. I. Preliminary observations. *Am J Bot*, **75**, 990-995. https://doi.org/10.2307/2443766

Smith-Moritz, A.M., Hao, Z., Fernandez-Nino, S.G., Fangel, J.U., Verhertbruggen, Y., Holman, H.Y.N., Willats, W.G.T., Ronald, P.C., Scheller, H.V., Heazlewood, J.L. and Vega-Sanchez, M.E. (2015) Structural characterization of a mixed-linkage glucan deficient mutant reveals

alteration in cellulose microfibril orientation in rice coleoptile mesophyll cell walls. *Front Plant Sci*, **6**, 628. https://doi.org/10.3389/fpls.2015.00628

Suslov, D. and Verbelen, J.P. (2006) Cellulose orientation determines mechanical anisotropy in onion epidermis cell walls. *J Exp Bot*, **57**, 2183-2192. https://doi.org/10.1093/jxb/erj177

Swarup, R., Kramer, E.M., Perry, P., Knox, K., Leyser, H.M., Haseloff, J., Beemster, G.T., Bhalerao, R. and Bennett, M.J. (2005) Root gravitropism requires lateral root cap and epidermal cells for transport and response to a mobile auxin signal. *Nat Cell Biol*, **7**, 1057-1065. https://doi.org/10.1038/ncb1316

Tomos, A.D., Malone, M. and Pritchard, J. (1989) The biophysics of differential growth. *Environ Exp Bot*, **29**, 7-23. https://doi.org/10.1016/0098-8472(89)90035-X

Tsai, S.W., Hahn, H.T. (1980) Introduction to composite materials. Routledge, New York.

Vega-Sanchez, M.E., Verhertbruggen, Y., Christensen, U., Chen, X.W., Sharma, V., Varanasi, P., Jobling, S.A., Talbot, M., White, R.G., Joo, M., Singh, S., Auer, M., Scheller, H.V. and Ronald, P.C. (2012) Loss of cellulose synthase-like f6 function affects mixed-linkage glucan deposition, cell wall mechanical properties, and defense responses in vegetative tissues of rice. *Plant Physiol*, **159**, 56-69. https://doi.org/10.1104/pp.112.195495

Verbelen, J.P., De Cnodder, T., Le, J., Vissenberg, K. and Baluska, F. (2006) The root apex of Arabidopsis thaliana consists of four distinct zones of growth activities: meristematic zone, transition zone, fast elongation zone and growth terminating zone. *Plant Signal Behav*, **1**, 296-304. https://doi.org/10.4161/psb.1.6.3511

Verhertbruggen, Y., Marcus, S.E., Haeger, A., Ordaz-Ortiz, J.J. and Knox, J.P. (2009) An extended set of monoclonal antibodies to pectic homogalacturonan. *Carbohyd Res*, **344**, 1858-1862. https://doi.org/10.1016/j.carres.2008.11.010

Vogler, H., Draeger, C., Weber, A., Felekis, D., Eichenberger, C., Routier-Kierzkowska, A.L., Boisson-Dernier, A., Ringli, C., Nelson, B.J., Smith, R.S. and Grossniklaus, U. (2013) The pollen tube: a soft shell with a hard core. *Plant J*, **73**, 617-627. https://doi.org/10.1111/tpj.12061

Wang, T., Chen, Y., Tabuchi, A., Cosgrove, D.J. and Hong, M. (2016) The target of beta-expansin expb1 in maize cell walls from binding and solid-state NMR studies. *Plant Physiol*, **172**, 2107-2119. https://doi.org/10.1104/pp.16.01311

Willats, W.G., Orfila, C., Limberg, G., Buchholt, H.C., van Alebeek, G.J., Voragen, A.G., Marcus, S.E., Christensen, T.M., Mikkelsen, J.D., Murray, B.S. and Knox, J.P. (2001) Modulation of the degree and pattern of methyl-esterification of pectic homogalacturonan in plant cell walls. Implications for pectin methyl esterase action, matrix properties, and cell adhesion. *J Biol Chem*, **276**, 19404-19413. https://doi.org/10.1074/jbc.M011242200

Willats, W.G., McCartney, L., Steele-King, C.G., Marcus, S.E., Mort, A., Huisman, M., van Alebeek, G.J., Schols, H.A., Voragen, A.G., Le Goff, A., Bonnin, E., Thibault, J.F. and Knox, J.P. (2004) A xylogalacturonan epitope is specifically associated with plant cell detachment. *Planta*, **218**, 673-681. https://doi.org/10.1007/s00425-003-1147-8

Wu, Y.J., Spollen, W.G., Sharp, R.E., Hetherington, P.R. and Fry, S.C. (1994) Root-growth maintenance at low water potentials - increased activity of xyloglucan endotransglycosylase and its possible regulation by abscisic-acid. *Plant Physiol*, **106**, 607-615. https://doi.org/10.1104/pp.106.2.607

Zerzour, R., Kroeger, J. and Geitmann, A. (2009) Polar growth in pollen tubes is associated with spatially confined dynamic changes in cell mechanical properties. *Dev Biol*, **334**, 437-446. https://doi.org/10.1016/j.ydbio.2009.07.044

Zhang, T., Tang, H., Vavylonis, D. and Cosgrove, D.J. (2019) Disentangling loosening from softening: insights into primary cell wall structure. *Plant J*, **100**, 1101-1117. https://doi.org/10.1111/tpj.14519

Zhang, Y., Yu, J., Wang, X., Durachko, D.M., Zhang, S. and Cosgrove, D.J. (2021) Molecular insights into the complex mechanics of plant epidermal cell walls. *Science*, **372**, 706-711. https://doi.org/10.1126/science.abf2824